4802 *Inorg. Chem.* **2010**, *49*, 4802–4813
DOI: 10.1021/ic9012075

Inorganic Chemistry
Article

Effects of Solvation on the Spin State of Iron(III) in 2,8,12,18-Tetrabutyl-3,7,13,17-tetramethyl-5,10-diazaporphyrinatoiron(III) Chloride

Pavel A. Stuzhin,*,† Sergei E. Nefedov,‡ Roman S. Kumeev,§ Anwar Ul-Haq,† Vadim V. Minin,‡ and Svetlana S. Ivanova†

†*Department of Organic Chemistry, Ivanovo State University of Chemical Technology, Friedrich Engels Pr-t, 7, RF-153000 Ivanovo, Russia*, ‡*N. S. Kurnakov Institute of General and Inorganic Chemistry RAS, Leninskij Pr-t, 31, RF-119991 Moscow, Russia*, and §*Institute of Solution Chemistry RAS, ul. Akademicheskaja, 1, RF-153045 Ivanovo, Russia.*

Received June 23, 2009

The chloroiron(III) complex of 2,8,12,18-tetrabutyl-3,7,13,17-tetramethyl-5,10-diazaporphyrin, [(Cl)FeMBDAP], was prepared and studied by X-ray crystallography and by solution ^{1}H NMR and UV−vis measurements. In the crystal structure of hemisolvate [(Cl)FeMBDAP] × 0.5$CHCl_3$, two nonequivalent [(Cl)FeMBDAP] units containing Fe1 and Fe2 are arranged in π-dimers with considerable overlap on their concave sides. Axial chloride bonded to Fe2 is solvated by hydrogen bonding with $CHCl_3$. Parameters of the coordination pyramid have typical values for the spin-mixed (S = 3/2 ÷ 5/2) Fe^{III} complexes in the case of Fe1 and are characteristic for the pure intermediate-spin state for Fe2 (displacement from the $(N_{Pyr})_4$ planes − 0.385 and 0.290 Å and the average N_{Pyr}−Fe bond lengths −1.992 and 1.954 Å for Fe1 and Fe2, respectively). Effective magnetic moments in $CHCl_3$ and CH_2Cl_2 capable of specific solvation of chloride by hydrogen bonding (4.5−4.6 μ_B at 298 K) are indicative about mixed intermediate/high-spin state S = 3/2 ÷ 5/2, with the S = 3/2 contribution increasing upon lowering of the temperature (4.02 μ_B in CD_2Cl_2 at 193 K). In nonsolvating CCl_4, C_6D_6, and THF-d_8, the μ_{eff} values are consistent with the predominantly high-spin state at ambient temperature (5.5−5.75 μ_B at 298 K) and almost pure S = 5/2 state at low temperature (ca. 5.9 μ_B in THF-d_8 below 270 K). Downfield isotropic shifts from 35 to 50 ppm are observed for α-alkyl protons and upfield shifts from −5 to −15 ppm for *meso*-CH protons, which is characteristic for the presence of the intermediate-spin state. The splitting of signals of the diastereotopic α-CH_2 protons is increased with growth of the S = 3/2 state contribution from 1.5 to 4 ppm in nonsolvating to 11 ppm in specifically solvating solvents at 298 K and further to 31 ppm at 193 K (in CD_2Cl_2). In the presence of DMSO addition and in methanol solution, the single CH_2 signal is observed at 25−28 ppm, and the *meso*-CH resonance is also shifted downfield to ca. 30 ppm, indicating the formation of six-coordinated complexes $[(DMSO)_2FeMBDAP]^+$ and $[(MeOH)_2FeMBDAP]^+$, the latter having the μ_{eff} value of 4.92 μ_B at 291 K is a spin-mixed species. The electron spin resonance spectra recorded at 77 K indicates that in frozen glasses in CD_2Cl_2 and THF molecules in the high-spin state ($g_\perp \sim 6$) and the predominantly intermediate-spin state ($g_\perp \sim 4.2$−4.3) coexist together.

Introduction

The spin state of Fe^{III} in five-coordinated complexes with porphyrins is strongly dependent on the nature of axial and macrocyclic ligands.[1,2] Thus, the chloroiron(III) complexes of β-octaethylporphyrin, [(Cl)FeOEP],[3] and *meso*-tetraphenylporphyrin, [(Cl)FeTPP],[4] are high-spin S = 5/2 species, whereas the corresponding complexes with weakly coordinating perchlorate [(ClO_4)FeTPP] and [(ClO_4)FeOEP] have a quantum mechanically mixed S = 3/2 ÷ 5/2 spin state.[5−8] Substitution of four *meso*-CH bridges in the porphyrin macrocycle by four *meso*-nitrogen atoms leads to stabilization of the intermediate-spin state S = 3/2, which is present in the Fe^{III} complexes of β-octaethyl-*meso*-tetraazaporphyrin [(X)FeOETAP] not only with a variety of weakly coordinating anions (X^- = ClO_4^-, CF_3COO^-, PF_6^-, SbF_6^-)[9] but also with chloride in [(Cl)FeOETAP].[10]

*Corresponding author. Telephone: +7 4932 477765. E-mail: stuzhin@isuct.ru.

(1) Scheidt, W. R.; Reed, C. A. *Chem. Rev.* **1981**, *81*, 543–555.
(2) Cheng, R. J.; Chen, P.-Y. *Chem.—Eur. J.* **1999**, *5*, 1708–1713.
(3) Ernst, J.; Subramanian, J.; Fuhrhop, J.-H. *Z. Naturforsch.* **1977**, *32A*, 1129-1136.
(4) Hoard, J. L.; Cohen, G. H.; Glick, M. D. *J. Am. Chem. Soc.* **1967**, *89*, 1992-1996.
(5) Dolphin, D. H.; Sams, J. R.; Tsin, T. B. *Inorg. Chem.* **1977**, *16*, 711.
(6) Hoff, H.; Shimomura, E. *J. Am. Chem. Soc.* **1980**, *102*, 31–37.
(7) Reed, C. A.; Mashiko, T.; Bentley, S. P.; Kastner, M. E.; Scheidt, W. R.; Spartalian, K.; Lang, G. *J. Am. Chem. Soc.* **1979**, *101*, 2948–2958.
(8) Dugad, L. B.; Mitra, S. *Proc.−Indian Acad. Sci., Chem. Sci.* **1984**, *93* (3), 295–311.
(9) Fitzgerald, J. P.; Yap, G. P. A.; Rheingold, A. L.; Brewer, C. T.; May, L.; Brewer, G. A. *J. Chem. Soc., Dalton Trans.* **1996**, 1249–1253.

 Published on Web 04/26/2010

Chart 1. Molecular Formula of Five-Coordinated Fe^{III} β-Octaalkylporphyrins with Different Degrees of *meso*-Azasubstitution

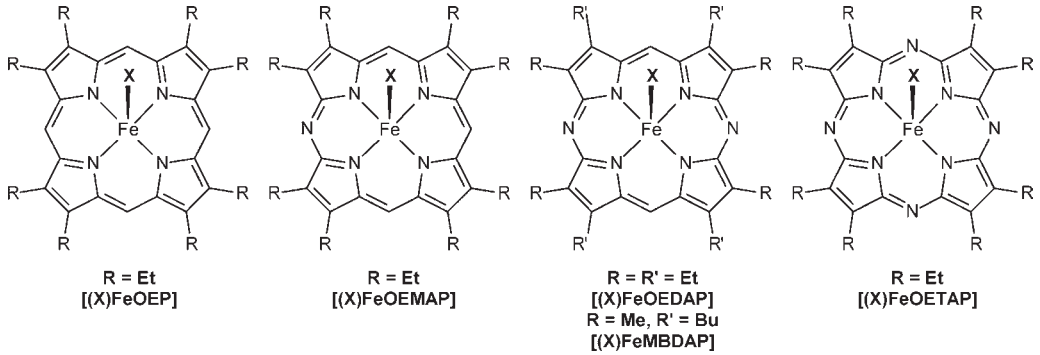

One can assume that change of the spin state of Fe^{III} in the five-coordinated complexes from $S = 5/2$ to 3/2 upon *meso*-tetraazasubstitution in the porphyrin macrocycle can originate from the decrease of the coordination cavity strengthening the σ-bonding with d_{x2-y2} orbitals and/or can be due to an increase of the π-acceptor properties of the macrocycle, leading to stabilization of lower lying d_π orbitals. Consideration of the effect of gradual *meso*-azasubstitution might be very helpful for a better understanding. In the case of the *meso*-monoazasubstituted derivative [(Cl)FeOEMAP] (Chart 1), the high-spin state was assigned[11] on the basis of the displacement of Fe from the N_4 plane (0.49 Å), solution magnetic moment of 5.7 μ_B at room temperature (RT) in the CH_2Cl_2 and ESR parameters ($g_\perp = 5.8$ and $g_\parallel = 2.0$ at 5 K in frozen CH_2Cl_2). The presence of one *meso*-nitrogen atom leads to some difference in two components of $g_\perp$, and it was noticed[12] in the electron spin resonance (ESR) spectrum recorded in frozen THF at 77 K ($g_x = 5.93$ and $g_y = 5.86$). Some deviation of the perpendicular components in the ESR spectra from the theoretical high-spin value of $g_\perp = 6$ was interpreted as an evidence of ca. 6% contribution of the intermediate-spin state. The Mössbauer parameters ($\delta_{Fe} = 0.27$ mm/s and $\Delta E_Q = 1.04$ mm/s)[12] are also in agreement with the $S = 5/2$ state. For the *meso*-diazasubstituted complex [(Cl)FeOEDAP] on the basis of the ESR spectrum in frozen THF ($g_x = 5.93$ and $g_y = 5.76$) and Mössbauer parameters ($\delta_{Fe} = 0.25$ mm/s and $\Delta E_Q = 1.54$ mm/s), the conclusion was made about the mixed spin state $S = 3/2 \div 5/2$, with ca. 8% contribution of the $S = 3/2$ state.[13,14] In the present work, we have prepared the chloroiron(III) complex of 2,8,12,18-tetrabutyl-3,7,13,17-tetramethyl-5,10-diazaporphyrin, [(Cl)FeMBDAP], and from the single crystal X-ray diffraction study, solution ^{1}H NMR, and ESR measurements we received evidence that contribution of the intermediate-spin state can be more substantially strong, depending on the solvent and temperature. *meso*-Diazaporphyrins combining methyl and butyl substituents in pyrrole rings have good solubility and are well suitable for solution study. Previously we have elaborated the synthesis of the free-base, H_2MBDAP,[15] and studied its complexes with copper(II), [CuMBDAP],[16] and indium(III), [(Cl)InMBDAP].[17] Recently we have preliminarily reported the structure of the μ-oxodiiron(III) species μ-O[FeMBDAP]$_2$,[18] and the study of the cationic six-coordinated low-spin Fe^{III} complexes $[(L)_2$FeMBDAP$]^+$ have been published by Japanese authors.[19]

Results and Discussion

The chloroiron(III) complex [(Cl)FeMBDAP] was obtained from the corresponding free base H_2MBDAP[15] and iron powder in glacial acetic acid under reflux, followed by treatment with aqueous HCl. Evaporation of solutions in $CHCl_3$ or crystallization by diffusion of hexane leads to black-brown needles which cannot be used for structural study. Crystals suitable for X-ray diffraction study were grown from a $CHCl_3$−heptane solution as a hemisolvate [(Cl)FeMBDAP] × 0.5$CHCl_3$. The molecular structure and crystal packing are presented in Figure 1.

Crystal Structure. The crystal structure is built up from two nonequivalent [(Cl)FeMBDAP] molecules containing Fe1 and Fe2 atoms. The Fe atoms are located above the mean planes formed by four-coordinating N_{Pyr} atoms, and the pyrrole rings form dihedral angles 0.5−3.0° with the corresponding $(N_{Pyr})_4$ plane. This leads to a slight dome conformation of the macrocycle which is additionally distorted by folding along the $N_{meso}\cdots N_{meso}$ axis in the Fe1 unit and along the $C_{meso}\cdots C_{meso}$ axis in the Fe2 unit. As a result, most of the pyrrolic C_β atoms are deviated from the mean $(N_{Pyr})_4$ planes in the direction opposite to the Fe atoms up to 0.1 Å. Molecules containing Fe1 and Fe2 are arranged in π-dimers with considerable overlap on their concave sides (Figure 2). The closest intermolecular distances between

(10) Fitzgerald, J. P.; Haggerty, B. S.; Rheingold, A. L.; May, L.; Brewer, G. A. *Inorg. Chem.* **1992**, *31*, 2006–2013.
(11) Balch, A. L.; Olmstead, M. M.; Safari, N. *Inorg. Chem.* **1993**, *32*, 291–296.
(12) Dzilin'ski, K.; Sinyakov, G. N.; Shul'ga, A. M. *Zh. Prikl. Spektrosk.* **1999**, *66*(4), 515−518; *J. Appl. Spectrosc.* **1999**, *66*, 566−569.
(13) Kaczmarzyk, T.; Dzilinski, K. *Nowe Technologie i Osiagniecia w Metalurgii i Inzynierii Materialowej, Miedzynarodowa Sesja Naukowa, 4th, Czestochowa, Poland*, **2003**, 505-508 (Pol.).
(14) Dzilinski, K.; Kaczmarzyk, T.; Jackowski, T.; Sinyakov, G. N.; Egorova, G. D. *Mol. Phys. Rep.* **2003**, *37*, 35–41.
(15) Khelevina, O. G.; Chizhova, N. V.; Stuzhin, P. A.; Semeikin, A. S.; Berezin, B. D. *Zh. Fiz. Khim.* **1997**, *71*, 81−85; *Russ. J. Phys. Chem.* **1997**, *71*, 74−78.
(16) (a) Khelevina, O. G.; Chizhova, N. V.; Stuzhin, P. A.; Semeikin, A. S.; Berezin, B. D. *Koord. Khim.* **1996**, *22*, 866-869; *Russ. J. Coord. Chem.* **1996**, *22*, 807−814. (b) Ogata, H.; Fukuda, T.; Nakai, K.; Fujimura, Y.; Neya, S.; Stuzhin, P. A.; Kobayashi, N. *Eur. J. Inorg. Chem.* **2004**, 1621–1629.
(17) (a) Stuzhin, P. A.; Goeldner, M.; Homborg, H.; Semeikin, A. S.; Migalova, I. S.; Wolowiec, S. *Mendeleev Commun.* **1999**, 134–136. (b) Stuzhin, P. A.; Ivanova, S. S.; Migalova, I. S. *Zh. Obshch. Khim.* **2004**, *74*, 1546−1556; *Russ. J. Gen. Chem.* **2004**, *74*, 1435−1445.
(18) Ul-Haq, A.; Nefedov, S. E.; Stuzhin, P. A. *J. Porphyrins Phthalocyanines* **2008**, *12*, 731.
(19) Ohgo, Y.; Neya, S.; Uekusa, H.; Nakamura, M. *Chem. Commun.* **2006**, 4590–4592.

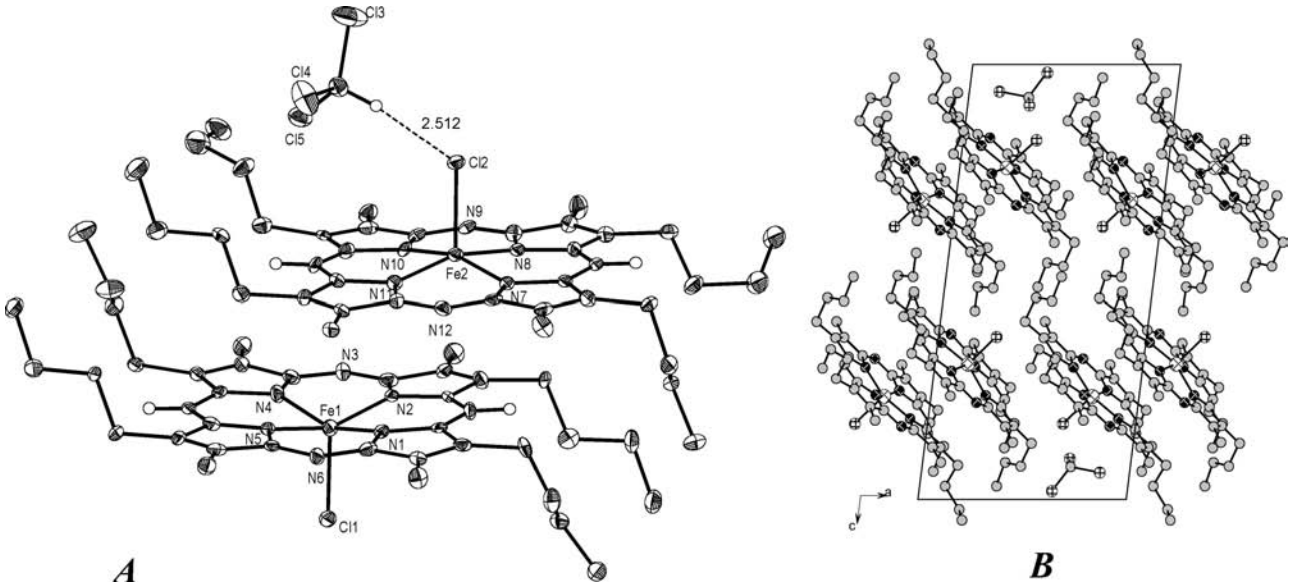

Figure 1. Molecular structure (*A*) and crystal packing (*B*) of [(Cl)FeMBDAP] × 0.5$CHCl_3$. For clarity, hydrogen atoms of the alkyl groups are omitted, and numbering is shown only for noncarbon atoms. The thermal ellipsoids are shown at 30% probability. Selected interatomic distances (Å) and angles (°): Fe1−Cl1 2.263(7), Fe1−N1 1.990(6), Fe1−N2 1.989(8), Fe1−N4 2.004(10), Fe1−N5 1.983(8), Fe2−Cl2 2.314(7), Fe2−N7 1.959(9), Fe2−N8 1.955(9), Fe2−N10 1.955(9), Fe2−N11 1.948(9), Fe1−Fe2 5.138(9).

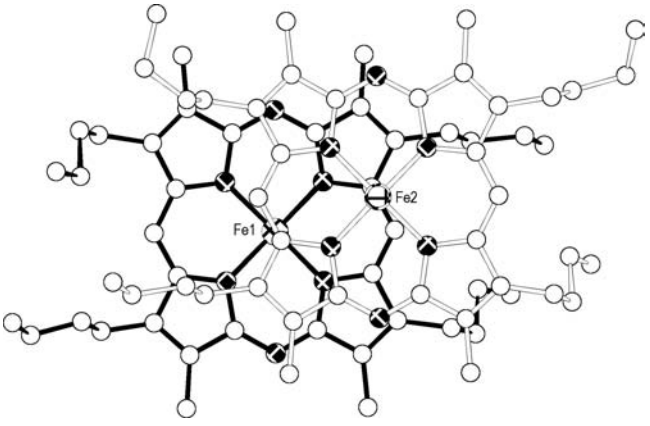

Figure 2. Molecular overlap in π-dimers of [(Cl)FeMBDAP].

atoms of two neighboring macrocycles in the π-dimer unit are 3.4−3.5 Å (e.g., C17···C58, 3.380(14); N3···C61, 3.414(14); and C4···N12, 3.424(14) Å). The values of interplane separation (3.387 Å), the distance between centers of two macrocycles ($C_t \cdots C_t'$ 4.627 Å), and their lateral shift (3.152 Å), according to classification suggested by Scheidt,[20] correspond to strong to intermediate $\pi-\pi$ interaction in the dimer unit. In the crystal packing, the π-dimeric units are arranged in stacks on their convex sides (Figure 1*B*). Only C_{meso} and C_β atoms on the edges of adjacent π-dimer units are overlapped with the shortest intermolecular interatomic contacts $C_{meso} \cdots C_{meso}'$ (C48···C29, 3.371(15) Å) and $C_\beta \cdots C_\beta'$ (C42···C31, 3.457(15); and C50···C23, 3.466(15) Å). Although the interplane separation between macrocycles on their convex sides is only 3.27 Å, a very large value of the lateral shift (7.39 Å) allows only a very weak $\pi-\pi$ convex−convex interaction.

Substitution of two *meso*-CH bridges by *meso*-N atoms leads to shortening of the $C_\alpha-X_{meso}$ bonds formed by a bridging *meso*-atom, from 1.37 to 1.38 Å to 1.32 to 1.33 Å, and decreases the $C_\alpha X_{meso} C_\alpha$ angle from 125° to 122° and increases the $X_{meso} C_\alpha N_{Pyr}$ angle from 124 to 125° to 127 to 128° (see Table 1). As a result, the radius of coordination cavity ($N_{Pyr} \cdots C_t$ distance: 1.954 Å for Fe1 and 1.933 Å for Fe2 units) is decreased, as compared to typical values of ca. 2.02 Å for the high-spin Fe^{III} porphyrin complexes.[1] This decrease of the coordination cavity is less pronounced than in the case of tetraazasubstituted species [(X)FeOETAP] (1.90 Å),[9,10] forming purely intermediate-spin Fe^{III} complexes. The average $N_{Pyr}-Fe$ bond lengths (1.992 and 1.954 Å for Fe1 and Fe2, respectively) are shorter than for the high-spin Fe^{III} porphyrins (2.05−2.07 Å)[1] and more close to the spin-mixed species (e.g., 1.994 Å for [(ClO_4)-FeOEP])[21] and the intermediate-spin Fe^{III} tetraazaporphyrins (1.91 and 1.93 Å for [(Cl)FeOETAP] and [(ClO_4)-FeOETAP], respectively).[9,10]

The withdrawal of the Fe1 and Fe2 atoms from the $(N_{Pyr})_4$ planes (0.385 and 0.290 Å, respectively) is close to the value typical for the intermediate spin Fe^{III} complexes of tetraazaporphyrin (0.26−0.35 Å)[9,10] and the spin-mixed Fe^{III} porphyrins (0.26−0.28 Å),[1] but is on the limit or less than usually observed for the high-spin Fe^{III} porphyrins (0.39−0.54 Å).[1] Therefore, structural parameters of crystalline [(Cl)FeMBDAP] are typical for the presence of the intermediate-spin state of Fe^{III}. It is noteworthy that geometry of coordination pyramids containing Fe1 and Fe2 is noticeably different and indicates a much stronger contribution of the $S = 3/2$ state in the case of Fe2. This difference results from the presence of a solvating molecule of $CHCl_3$ which forms a hydrogen bond with the axial chlorine atom Cl2 bonded with Fe2. The distance Cl2···$HCCl_3$ is 2.512 Å, which is close to the mean value of of 2.39 Å reported for the hydrogen bond between chloride and $CHCl_3$ in organo-(metallic) crystal structures.[22] The hydrogen (H)-bonding

(20) Scheidt, W. R.; Lee, Y. J. *Struct. Bonding* (*Berlin, Ger.*) **1987**, *64*, 1–70.
(21) Masuda, H.; Taga, T.; Osaki, K.; Sugimoto, H.; Yishida, Z.-I.; Ogoshi, H. *Inorg. Chem.* **1980**, *19*, 950–955.

Table 1. Selected Average Geometric Parameters for Five-Coordinated Fe^{III} Complexes of Porphyrins and *meso*-Azaporphyrins

	[(X)FeOEP]			[(Cl)FeMBDAP]		[(X)FeOETAP]	
geometric parameter	ClO_4	Cl	[(Cl)FeOEMAP]	Fe1	Fe2	ClO_4	Cl
$C_\alpha-X_{meso}$			1.361 (N)	1.328	1.323		1.320
	1.363	1.378	1.375 (C)	1.371	1.378		
$C_\alpha-N_{Pyr}$	1.394	1.384	1.377	1.377	1.383		1.383
$C_\alpha-C_\beta$	1.416	1.453	1.448	1.453	1.441		1.456
$C_\beta-C_\beta$	1.397	1.358	1.359	1.352	1.347		1.362
$N_{Pyr}-C_t$	1.977	2.010	1.984	1.954	1.933	1.895	1.897
$Fe-C_t$	0.26	0.463	0.49	0.385	0.290	0.263	0.352
Fe−X	2.067	2.231	2.254	2.263	2.314	2.091	2.278
$Fe-N_{Pyr}$	1.994	2.063	2.044	1.992	1.954	1.913	1.929
$\angle C_\alpha X_{meso} C_\alpha$			124.3 (N)	121.5 (N)	122.1		121.3
	126.4	126.9	125.6 (C)	124.8 (C)	125.4		
$\angle C_\alpha N_{Pyr} C_\alpha$	105.1	105.6	105.5	106.3	104.6		107.5
$\angle X_{meso} C_\alpha N_{Pyr}$			125.5 (N)	128.0	126.9		128.1
	124.3	124.3	124.9 (C)	125.0	123.8		
ref	21	3	11	this work	this work	9	10

Table 2. Solution Magnetic Moments (μ_B) for [(Cl)FeMBDAP]

solvent	T, K	magnetic moment, μ_B	% of $S = 3/2$	solvent	T, K	magnetic moment, μ_B	% of $S = 3/2$
CD_2Cl_2	298	4.71	64	C_6D_6	298	5.59	19
	273	4.50	74	THF-d_8	323	5.61	18
	253	4.46	75		297	5.70	13
	233	4.34	81		273	5.90	1
	213	4.19	87		253	5.92	0
	193	4.02	94		233	5.83	5
$CDCl_3$	298	4.62	68		213	5.92	0
CCl_4	298	5.64	16		193	5.87	3
CD_3OD	291	4.92	54	acetone-d_6	294	5.50	24

of the axial chloride with $CHCl_3$ leads to weakening and elongation of the Fe−Cl bond (2.314 vs 2.263 Å for Fe2 and Fe1, respectively) and consequent stabilization of the $S = 3/2$ state.

We have supposed that such an effect of solvation on the spin state of Fe^{III} should be observed not only in the crystalline state but also in solution. This was indeed demonstrated by results of magnetic, ^1H NMR, and ESR studies of [(Cl)FeMBDAP] in noncoordinating solvents having different abilities to specific solvation of the chlorine atom.

Effective Magnetic Moments. Effective magnetic moments (μ_{eff}) were measured using a NMR technique by Evans method[23,24] for solutions of [(Cl)FeMBDAP] in different solvents at room and low temperatures (Table 2). In the solvents with poor or lacking H-bonding abilities (acetone-d_6, C_6D_6, CCl_4, THF-d_8), the room temperature μ_{eff} values (5.5−5.7 μ_B) are slightly lower than that of the spin-only value for the high-spin Fe^{III} complexes ($\mu_{HS} = 5.92\,\mu_B$). In CD_2Cl_2 and $CDCl_3$, which due to their more pronounced CH acidity are capable of specific solvation of an axial chlorine atom, the μ_{eff} values at 298 K are much lower (4.6−4.7 μ_B). Similar RT μ_{eff} values have been observed for the spin-mixed ($S = 3/2 \div 5/2$) Fe^{III}−porphyrin complexes[25] [(ClO_4)FeOEP] (4.79 μ_B at 293 K) and [(ClO_4)FeTPP] (5.05 μ_B at 293 K for the solid sample and 4.8 μ_B at 299 K in $CDCl_3$ solution).

Temperature dependence of the magnetic moment has been studied for the [(Cl)FeMBDAP] solutions in THF-d_8 (193−323 K) and in CD_2Cl_2 (193−298 K). In nonsolvating THF-d_8, the μ_{eff} value slightly increases at low temperatures and below 273 K becomes practically constant (5.8−5.9 μ_B) and characteristic for the pure $S = 5/2$ spin state. In contrast to that in solvating CD_2Cl_2, the μ_{eff} value gradually decreases upon lowering of the temperature from 4.71 μ_B at 298 K to 4.02 μ_B at 193 K, closely approaching the spin-only value for the purely intermediate $S = 3/2$ spin state Fe^{III} complexes ($\mu_{IS} = 3.87\,\mu_B$). It should be noted, that for the purely high-spin Fe^{III}−porphyrin complexes, the magnetic moment is nearly constant above 100 K and close to the spin-only value for the $S = 5/2$ state: μ_{eff} values for solid [(Cl)FeOEP] are 5.81 μ_B at 297 K and 5.78 μ_B at 160 K[3] and for solid [(Cl)FeTPP] are 5.83 μ_B at 293 K and 5.81 at 194 K.[26] For the purely intermediate spin Fe^{III}−tetraazaporphyrin complex [(Cl)FeOETAP],[9] the magnetic moment is also practically independent from the temperature above 100 K and close to the spin-only value for the $S = 3/2$ state (μ_{eff} is ca. 3.90−3.94 μ_B for solid sample). For the spin-mixed Fe^{III}−porphyrin complexes ($S = 3/2 \div 5/2$), the magnetic moment is temperature dependent[25] and approaches the $S = 3/2$ spin-only value only near 10 K. Thus, for the solid samples [(ClO_4)FeOEP] and [(ClO_4)FeTPP], the μ_{eff} value is decreased from 4.79 and 5.05 μ_B at 293 K to 4.42 and 4.79 μ_B at 178 K, respectively. In $CDCl_3$ solution of [(ClO_4)FeTPP], the μ_{eff} value is lower than in the solid state and decreased from 4.8 μ_B at 299 K to 4.3 μ_B at 215 K.[6]

(22) Steiner, T. *Acta Crystallogr., Sect. B: Struct. Sci.* **1998**, *54*, 456–463.
(23) Evans, D. F. *J. Chem. Soc.* **1959**, 2003.
(24) Braun, S.; Kalinowski, H.-O., Berger, S. *100 and More Basic NMR Experiments*. VCH: Weinheim, Germany, 1996; p 237−239.
(25) Mitra, S. In *Iron Porphyrins*; Lever, A. B. P., Gray, H. B., Eds.; Addison-Wesley: Boston, MA, 1983, Part *2*; pp 1−42.
(26) Maricondi, C.; Swift, W.; Straub, D. K. *J. Am. Chem. Soc.* **1969**, *91*, 5205.

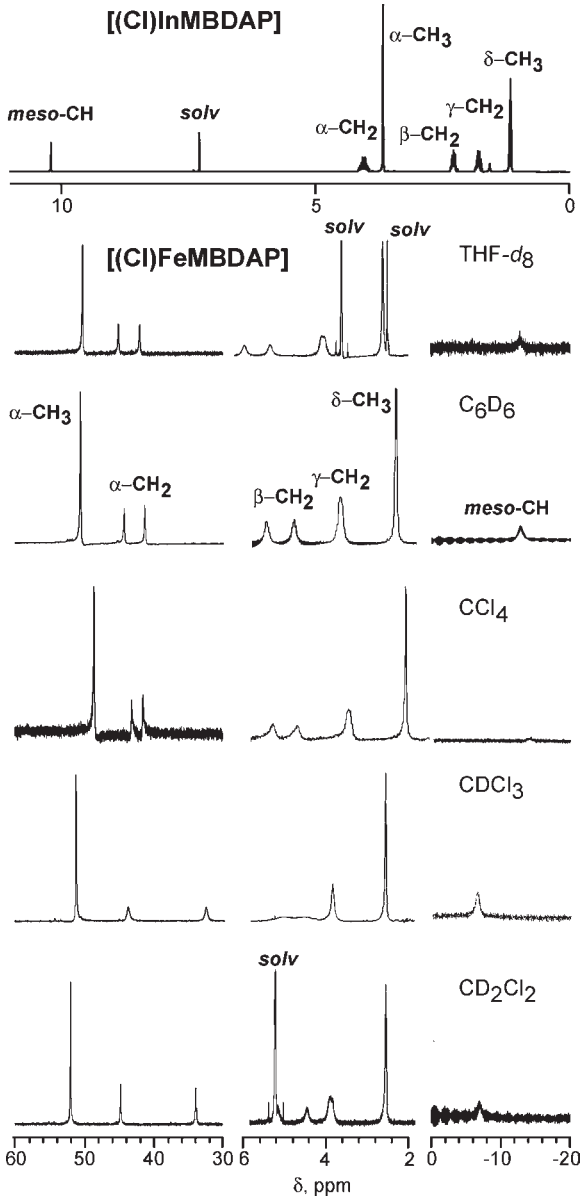

Figure 3. ^{1}H NMR spectra of [(Cl)FeMBDAP] in various solvents and [(Cl)InMBDAP] in $CDCl_3$ at 294 K.

Therefore results of our magnetic measurements indicate that [(Cl)FeMBDAP] is also a spin-admixed complex which, depending on the solvent and temperature, can exist predominantly in the high- or intermediate-spin states. The contribution of the intermediate spin-state can be roughly estimated from the measured μ_{eff} values as $(\mu_{HS}^2 - \mu_{eff}^2)/(\mu_{HS}^2 - \mu_{IS}^2)$. At ambient temperature (290−300 K), [(Cl)FeMBDAP] is predominantly a high-spin species in nonsolvating THF-d_8, C_6D_6, CCl_4, and acetone-d_6 (ca. 15−25% of the $S = 3/2$ state) and has a predominantly intermediate spin in CD_2Cl_2 and $CDCl_3$ specifically solvating axial chloride (65−70% of the $S = 3/2$ state). At 193 K, [(Cl)FeMBDAP] exists in THF-d_8 as the almost pure high-spin complex (>95% of the $S = 5/2$ state) and in CD_2Cl_2 as almost pure intermediate-spin complex (94% of the $S = 3/2$ state).

^{1}H NMR Spectra. Paramagnetism of Fe^{III} leads to considerable shifts of signals in the ^{1}H NMR spectra of [(Cl)FeMBDAP] as compared to their position in the diamagnetic analogue, In^{III} complex [(Cl)InMBDAP][17] (see Figure 3 and Table 3). The most pronounced isotropic shifts $\Delta\delta = \delta_{para} - \delta_{dia}$ are observed for protons in the α-positions of alkyl groups (downfield shift from 3.5 to 4 ppm to 30 to 55 ppm, $\Delta\delta = 27-55$ ppm) and for *meso*-CH protons (upfield shift from 10 to 11 ppm to −6 to −15 ppm, $\Delta\delta = -15$ to −26 ppm). Such strong isotropic shifts are determined by σ- and/or π-contact mechanisms of spin delocalization. Smaller downfield shifts (1.5−3 ppm) for protons in the β-, γ-, and δ-positions of the butyl groups result from the dipole mechanism of spin delocalization.

In the Fe^{III} complexes having up to five singly occupied d orbitals, the direct delocalization of the spin density onto the porphyrin macrocycle with effective D_{4h} symmetry can occur only from the d_{x2-y2} and d_π orbitals, according to the σ- and π-contact mechanisms, respectively. Delocalization from the d_{x2-y2} orbital along the framework of σ-bonds is responsible for the large downfield shift observed for the resonances of the pyrrolic CH and α-alkyl protons in the high-spin Fe^{III} porphyrins.[27,28] Spin density from two degenerated d_π orbitals can be delocalized either by π-bonding interaction with the filled π-orbitals ($d_\pi \Leftarrow e_g(\pi)$) or by π-backbonding with the lowest unoccupied π-orbitals ($d_\pi \Rightarrow e_g(\pi^*)$). It was generally accepted that these π-spin delocalization pathways are responsible, respectively, for the downfield shift of the *meso*-CH resonances in the six-coordinated and their upfield shift in the five-coordinated high-spin Fe^{III} porphyrin complexes.[27,28] Recent theoretical works have shown that if the effective symmetry of the macrocycle is lowered from D_{4h} to D_{2d} by ruffling[29] or to C_{4v} by doming in the five-coordinated Fe^{III} complexes,[30,31] the spin density can be also delocalized onto the filled $a_{2u}(\pi)$ orbital from the d_{xy} and d_{z2} orbitals, respectively. This leads to the large spin density on the *meso*-C atoms and provides an alternative and probably more reasonable explanation of the large upfield shift of the *meso*-CH resonances in the five-coordinated high-spin Fe^{III} porphyrin complexes.[31]

The strong downfield isotropic shift observed for the α-CH_3 and α-CH_2 signals is typical for the five-coordinated Fe^{III} complexes of β-alkyl substituted porphyrins.[27,28] It is noteworthy that the splitting of the signal of the diastereotopic α-CH_2 protons strongly depends on the solvent nature. In CD_2Cl_2 and $CDCl_3$ capable to specific solvation of axial chloride, the value of splitting (ca. 11 ppm) is at least three times larger than that in nonsolvating C_6D_6, CCl_4, and THF-d_8 (1.5−4 ppm). Analysis of the available literature data on five-coordinated Fe^{III} porphyrins shows that the splitting of the α-CH_2 signal is

(27) Goff, H. M. In *Iron Porphyrins*; Lever, A. B. P.; Gray, H. B., Eds; Addison-Wesley: Boston, MA, 1983, Part *1*; pp 237−281.
(28) Walker, F. A. In *The Porphyrin Handbook*; Kadish, K. M., Smith, K. M., Guilard, R., Eds; Academic Press: Amsterdam, The Netherlands, 2000; Vol. *5*, pp 81−183.
(29) (a) Safo, M. K.; Walker, F. A.; Raitsimring, A. M.; Walters, W. P.; Dolata, D. P.; Debrunner, P. G.; Scheidt, W. R. *J. Am. Chem. Soc.* **1994**, *116*, 7760–7770. (b) Ghosh, A.; Gonzalez, E.; Vangberg, T. *J. Phys. Chem. B* **1999**, *103*, 1363–1367.
(30) Ghosh, A.; Vangberg, T.; Gonzalez, E.; Taylor, P. *J. Porphyrins Phthalocyanines* **2001**, *5*, 345–356.
(31) Cheng, R.-J.; Chen, P.-Y.; Lovell, T.; Liu, T.; Noodleman, L.; Case, D. A. *J. Am. Chem. Soc.* **2003**, *125*, 6774–6783.

Table 3. Proton Chemical Shifts (δ, ppm) for [(Cl)FeMBDAP] and Related In^{III} and Fe^{III} Complexes at 298 K

complex	solvent	α-CH_3	α-CH_2		β-$CH_{2(3)}$		γ-CH_2	δ-CH_3	*meso*-CH
[(Cl)InMBDAP]	$CDCl_3$	3.66	4.08	4.00	2.28		1.80	1.15	10.21
[(Cl)FeMBDAP]	CD_2Cl_2	52.02	44.79	33.97	hidden	4.57	4.01	2.65	−7.03
	$CDCl_3$	51.18	43.61	32.38	5.08	4.60	3.92	2.65	−6.54
	CCl_4	48.94	43.47	41.89	5.70	5.09	3.89	2.49	−14.6 br
	C_6D_6	50.67	44.36	41.34	5.61	4.93	3.81	2.47	−12.88
	THF-d_8	49.53	44.45	41.45	5.87	5.25	4.01 3.99	2.56	−13.01
	acetone-d_6	51.33	45.79	37.31	5.36	4.89	4.03 3.95	2.61	−11.63
	methanol-d_4	60.54	27.75		2.97		2.05	2.22	+30.2
[(Cl)FeEtioP][a]	$CDCl_3$	53	44	40	7.2				−51
[(ClO_4)FeEtioP][a]	$CDCl_3$	64	43	28	7				−11.4
[(Cl)FeOEP][b]	CD_2Cl_2		44.5	40.9	6.8				−56.8
[(ClO_4)FeOEP][b]	CD_2Cl_2		36.5		6.5				−6
[(Cl)FeOETAP][c]	$CDCl_3$		38.76	15.29	4.06				−

[a] Ref 6. [b] Ref 34. [c] Ref 10.

increased in the presence of the intermediate-spin state. In the purely high-spin complexes, its value is 3−4 ppm and does not depend on solvating abilities of the solvent (e.g., 3.6 ppm for [(Cl)FeOEP] both in C_7D_8 and in CD_2Cl_2).[32] The splitting is increased to ca. 17 ppm in the spin-mixed perchlorate complex [(ClO_4)FeEtioP][6] and in the purely intermediate spin Fe^{III} octaethyltetraazaporphyrin complex [(Cl)FeOETAP] reaches 23.7 ppm both in C_6D_6 and in $CDCl_3$.[10] Therefore, in line with the measured μ_{eff} values, the splitting of the α-CH_2 signal in [(Cl)-FeMBDAP] observed at ambient temperature is indicative of predominant high-spin state in nonsolvating and predominant intermediate-spin state in solvating H-bonding solvents. It is noteworthy, that effects of solvation of axial ligands with H-bonding solvents on the electronic structure of Fe^{III} in porphyrin complexes was observed previously only for the low-spin six-coordinated *bis*-cyano complexes of tetra-*meso*-(2,4,6-triethylphenyl)-porphyrinatoiron(III);[33] the $(d_{xy})^2(d_\pi)^3$ ground state in nonpolar solvents, such as toluene, benzene, and CCl_4 is changed to $(d_\pi)^4(d_{xy})^1$ in H-bonding solvents such as chloroform, dichloromethane, and methanol.

Lowering of temperature has distinctly different effects on the resonance position in the ^{1}H NMR spectra of [(Cl)FeMBDAP] solutions in THF-d_8 and CD_2Cl_2. Figure 4 illustrates the spectral changes observed for the α-alkyl protons, and Figure 5 shows the Curie plot (dependence of the isotropic shifts $\Delta\delta$ from $1/T$). In THF-d_8, lowering of temperature results in a noticeable downfield shift of all alkyl proton signals (Figure 4, left panel), while the *meso*-CH resonance is broadened and shifted slightly upfield. The dependence of the isotropic shifts from $1/T$ is almost linear in the investigated temperature range (Figure 5, left panel). This is typical for high-spin Fe^{III}−porphyrin complexes,[8,27,28] and some deviation from the Curie law is evidently due to dipolar contributions arising from the zero-field splitting of the ground state ($^6A_1$) and depending on $1/T^2$.

More complex nonlinear temperature dependence of the isotropic shifts is observed in CD_2Cl_2 (Figure 5, right panel). Unlike THF-d_8 in CD_2Cl_2, only α-CH_3 and one of α-CH_2 resonances are shifted downfield with lowering of the temperature, while the opposite upfield shift is

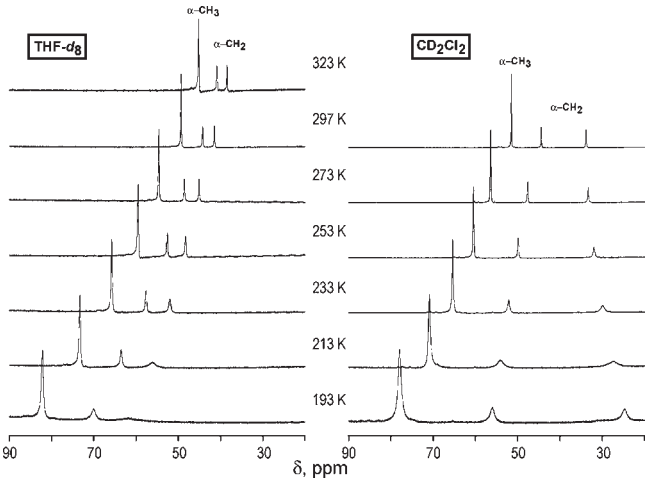

Figure 4. Effect of the temperature on the position of α-alkyl resonances in the ^{1}H NMR spectra of [(Cl)FeMBDAP] in THF-d_8 (left panel) and CD_2Cl_2 (right panel).

observed for another α-CH_2 resonance (Figure 4). Signals of both β-CH_2 and *meso*-CH protons are also shifted to the higher field at low temperatures, whereas signals of γ-CH_2 and δ-CH_3 protons appear only slightly temperature dependent (Figure 5, right panel).

The opposite temperature dependence for the signals of two diastereotopic α-CH_2 protons observed in CD_2Cl_2 leads to the most characteristic feature in the spectra evolution—the splitting of the α-CH_2 signals is strongly increased from 10.6 ppm at 298 K to 26.7 ppm at 213 K and reaches 31.3 ppm at 193 K. As it was mentioned above, such large splitting of the α-CH_2 resonances is typical for the presence of the $S = 3/2$ spin state in the five-coordinated Fe^{III}−porphyrin and Fe^{III}−tetraazaporphyrin complexes. For the spin-mixed complex [(ClO_4)FeEtioP] in the 300−215 K temperature range, the low-field component of the α-CH_2 resonance exhibits linear Curie behavior, and the high-field one does not depend on the temperature which results in the increase of splitting from 17 ppm at 299 K to ca. 25 ppm at 216 K.[6] Unlike this latter species, for [(Cl)FeMBDAP] with lowering of the temperature, the contribution of the intermediate-spin state is increased (see magnetic data above), and due to the changes in spin delocalization mechanism, this leads to the considerable curvature in the Curie plots in the 300−190 K range, especially for

(32) Morishima, I.; Kitagawa, S.; Matsuki, E.; Inubushi, T. *J. Am. Chem. Soc.* **1980**, *102*, 2429.
(33) Ikezaki, A.; Nakamura, M. *Inorg. Chem.* **2002**, *41*, 2761–2768.

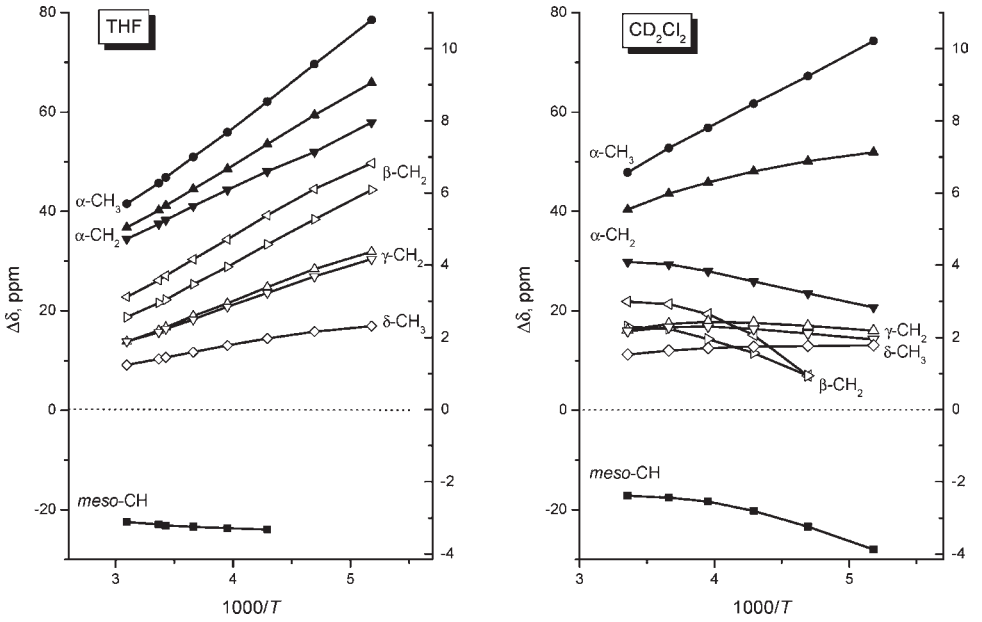

Figure 5. Temperature dependence of isotropic shifts in the ^{1}H NMR spectra of [(Cl)FeMBDAP] in THF-d_8 (left panel) and CD_2Cl_2 (right panel). On the each panel the black experimental points are linked to the left and white to the right axis.

α-CH_2, β-CH_2, and *meso*-CH protons (Figure 5, right panel).

The increase of the CH_2 splitting with the growth of the $S = 3/2$ spin-state contribution can be rationalized in terms of the spin delocalization mechanisms. For the five-coordinated $S = 5/2$ species, the strong downfield shift of α-alkyl resonances is primarily determined by the σ-spin delocalization from the d_{x2-y2} orbital. The σ-contact mechanism should have similar effect on both diastereotopic α-CH_2 protons, and some splitting of their resonances is due to some minor contribution of the π-contact and dipole mechanisms. In the intermediate-spin state $S = 3/2$, the d_{x2-y2} orbital is empty, and the downfield isotropic shift of the α-CH_3 and α-CH_2 resonances is determined only by π-contact and dipole mechanisms. Both of them have a differentiating effect on the resonances of the diastereotopic α-CH_2 protons, and their splitting is increased. Isotropic shifts for the β-CH_2, γ-CH_2, and δ-CH_3 signals are determined by dipole and σ-spin delocalization mechanisms. Decrease of the high-spin state contribution, weakening the effect of σ-spin delocalization from the d_{x2-y2} orbital, should decrease the downfield isotropic shift, especially for β-CH_2 protons. Indeed, at ambient temperature in the H-bonding solvents, the downfield isotropic shift for the β-CH_2 resonances is smaller than in nonsolvating solvents by 0.4−0.8 ppm, while position of γ-CH_2 and δ-CH_3 signals are similar (see Table 3). At 213 K, the observed downfield shifts in CD_2Cl_2 become noticeably smaller than in THF-d_8 by 4.3−5.8 ppm for β-CH_2, 1.6 ppm for γ-CH_2, and 0.4 ppm for δ-CH_3 signals. This is completely consistent with the results of magnetic moment measurements (see above) indicating that at low temperatures the high-spin state is maintained in nonsolvating THF-d_8, but in H-bonding CD_2Cl_2 its contribution is strongly decreased and the complex becomes almost purely intermediate spin species. Noteworthy that the dipole shift for the high-spin Fe^{III} is dependent on $1/T^2$, while for the intermediate spin Fe^{III} the dependence on $1/T$ should be linear.[28] These facts explain the observed curvature of the CH_2 resonances especially for the higher field α-CH_2 and both β-CH_2 resonances exhibiting distinct anti-Curie behavior in the investigated temperature range in CD_2Cl_2 (Figure 5, right panel).

The displacement of Fe^{III} from the porphyrin plane is decreased in going from the high- to the intermediate-spin state, and the effect of π-delocalization from the d_π orbitals onto the macrocyclic e_g orbitals should be enhanced, while from the d_{z2} onto $a_{2u}(\pi)$ orbital should be diminished. Since the $e_g(\pi)$ and $e_g(\pi^*)$ orbitals have both considerable contribution of β-pyrrolic C-atoms, which is larger than that of the $a_{2u}(\pi)$ orbital, it is difficult to elucidate the nature of the π-contact mechanism only from the behavior of the α-alkyl resonances. Analysis of the *meso*-CH shifts might be helpful because the $e_g(\pi^*)$ and $a_{2u}(\pi)$ orbitals have large coefficients on the *meso*-C atoms, unlike the $e_g(\pi)$ orbital which has nodes.

Although the isotropic upfield shift of the *meso*-CH protons is increased in going from specifically solvating CD_2Cl_2 and $CDCl_3$ (−6 to −7 ppm) to nonsolvating CCl_4, C_6D_6, and THF (−12 to −15 ppm), in both cases its value is much smaller than is typical for the high-spin Fe^{III} porphyrins (−50 to −60 ppm for [(Cl)FeEtioP] and [(Cl)FeOEP][6,27,32]) and close to the values for the spin-admixed perchlorate complexes of Fe^{III} porphyrins (−5 to −11 ppm for [(ClO_4)FeEtioP] and [(ClO_4)FeOEP]).[6,34] The decrease of the upfield isotopic shift for the predominantly high-spin species existing in nonsolvating solvents is due to the effect of *meso*-azasubstitution. In the case of high-spin Fe^{III} porphyrins, the upfield shift for *meso*-CH protons is explained by the π-contact mechanism of spin delocalization from the d_π orbitals to the degenerated $e_g(\pi^*)$ orbitals of the macrocycle[27,28] or alternatively by the $d_{z2} \Leftarrow a_{2u}(\pi)$ interaction.[31] In the high-spin [(Cl)FeMBDAP] both π-delocalization pathways should be diminished. Substitution of two opposite

(34) Kitner, E. T.; Dauson, J. H. *Inorg. Chem.* **1991**, *30*, 4892–4897.

meso-CH groups by *meso*-N atoms lifts the degeneracy of the $e_g(\pi^*)$ orbitals.[16b,35] Only one of them can participate in π-delocalization on *meso*-carbons: spin density from the d_{xz} orbital resides mainly on the more electronegative *meso*-N atoms of the lowest unoccupied molecular orbital (LUMO), which have nodes on the opposite *meso*-carbon atoms, while π-spin delocalization onto the *meso*-carbon atoms involves d_{yz} and LUMO+1. As a result, a high-field isotopic shift is strongly decreased for the *meso*-CH protons. At the same time *meso*-azasubstitution in porphyrins leads to considerable stabilization of the $a_{2u}(\pi)$ orbital,[35] and therefore, π-spin delocalization on *meso*-carbons through the $d_{z2} \Leftarrow a_{2u}(\pi)$ interaction becomes also less effective.

In the ^{1}H NMR spectrum reported for the high-spin *meso*-monoazasubstituted species [(Cl)FeOEMAP],[11] three *meso*-CH protons give two broad signals at ca. −26 and −18 ppm with a 2:1 ratio (in CD_2Cl_2 at RT). This is in line with the above explanations. The π-spin-density from the d_{xz} orbital is delocalized mainly on the *meso*-nitrogen atom of the LUMO and to a lesser extent on the opposite *meso*-carbon, delocalization from d_{yz} occurs equally on two opposite *meso*-carbon atoms of the LUMO+1. On the other hand, the stabilization of the $a_{2u}(\pi)$ type orbital is less in *meso*-monoaza- than in *meso*-diazasubstituted porphyrins, and consequently the π-spin delocalization by the $d_{z2} \Leftarrow a_{2u}(\pi)$ interaction in [(Cl)FeOEMAP] should be more effective than in the *meso*-diazasubstituted species but less effective than in Fe^{III} porphyrins. In general it should be noticed that, since *meso*-azasubstitution leads to stabilization of the $a_{2u}(\pi)$ and $e_g(\pi^*)$ type orbitals, strengthening π-acceptor and weakening π-donor properties of the tetrapyrrolic ligand,[16b,35] in the Fe^{III} complex of *meso*-diazaporphyrin the contribution of the $d_\pi \Rightarrow e_g(\pi^*)$ delocalization pathway should be increased with respect to $d_{z2} \Leftarrow a_{2u}(\pi)$.

The position of the *meso*-CH resonances in [(Cl)FeMBDAP] only slightly depends on the solvent nature and on the temperature, i.e., factors strongly influencing the contribution of the high and intermediate-spin states. The upfield isotropic shift of *meso*-CH resonances in nonsolvating solvents (−22 to −25 ppm) have almost negligible temperature dependence (−23 ppm at 297 K and −24 ppm at 233 K in THF-d_8). The values of the *meso*-CH isotropic shift in H-solvating solvents are slightly smaller at ambient temperature (−17 to −18 ppm at 298K), but at low temperature they are increased (−28 ppm in CD_2Cl_2 at 193 K) and become larger than in THF-d_8. This is unlike Fe^{III} porphyrins for which the upfield isotopic shift of the *meso*-CH resonance is strongly decreased in going from the high-spin complexes to the spin-mixed complexes (from −60 to −70 to −15 to −20 ppm). It was explained by switching of the π-spin delocalization mechanism from $d_\pi \Rightarrow e_g(\pi^*)$ to $d_\pi \Leftarrow e_g(\pi)$[28] or, alternatively, by weakening of the $d_{z2} \Leftarrow a_{2u}(\pi)$ interaction due to a decrease of the Fe^{III} withdrawal from the porphyrin plane.[31] The distinct anti-Curie behavior, which was observed for the *meso*-CH resonance in spin-mixed [(ClO_4)FeEtioP] (*meso*-CH resonance is shifted from −14 ppm at 327 K to −4 ppm at 238 K),[6] seems to be more consistent with the latter mechanism. The growth of the upfield *meso*-CH shift for [(Cl)FeMBDAP] in CD_2Cl_2 upon lowering of the temperature evidences that in this case the $d_\pi \Rightarrow e_g(\pi^*)$ spin delocalization is more important. This is in line with higher π-acceptor properties of *meso*-azasubstituted porphyrin macrocycle.

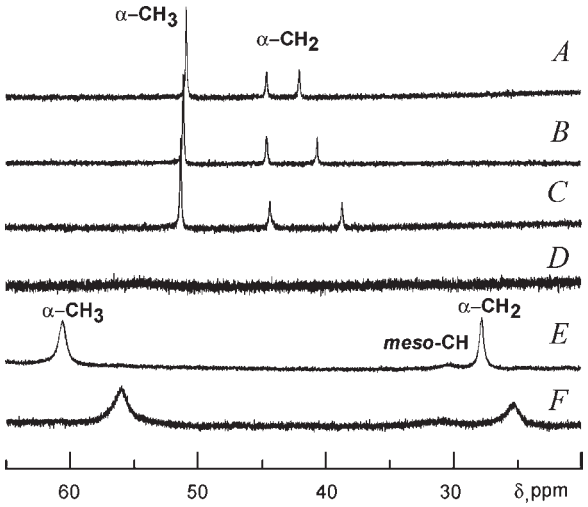

Figure 6. Low-field region of the ^{1}H NMR spectra of [(Cl)FeMBDAP] in C_6D_6 (*A*) and its changes after addition of CD_3OD − 1% (*B*), 6% (*C*), and 25% (*D*). Spectra of high-spin six-coordinated complexes [(CD_3OD)$_2$FeMBDAP]$^+$ in CD_3OD (*E*) and [(DMSO-d_6)$_2$FeMBDAP]$^+$ in $CDCl_3$/DMSO-d_6 4:1 (*F*). Spectra recorded at 298 K.

We have also studied the influence of the CD_3OD additions on the ^{1}H NMR spectra of [(Cl)FeMBDAP] in C_6D_6 (Figure 6, spectra *A*−*C*). Small additions increase the α-CH_2 splitting since H-bonding of the axial chloride with methanol leads to stabilization of the intermediate spin-state. The broad *meso*-CH resonance is shifted from −13 ppm to −10 ppm. At higher CD_3OD concentration, the α-alkyl and *meso*-CH signals are strongly broadened and cannot be observed (Figure 6, spectrum *D*). In pure CD_3OD the broadened α-CH_3 resonance is shifted upfield to 60.5 ppm, while α-CH_2 appears as singlet at 27.7 ppm (Figure 6, spectrum *E*). The *meso*-CH resonance is shifted from an upfield to a downfield region and gives a broad line at 30.2 ppm. Such spectral features are typical for the six-coordinated Fe^{III} complexes[28,32,36] and evidence the formation of [(CD_3OD)$_2$FeMBDAP]$^+$. The solution magnetic moment of 4.92 μ_B is consistent with the spin-mixed state with approximately equal intermediate- and high- spin contributions. The *bis*-alcohol complex [(CD_3OD)$_2$FeTPP]$^+$ was also supposed to be an intermediate- or mixed spin species,[28,37] while [(ROH)$_2$FeOEP]$^+$ is considered as a high-spin species.[32]

Addition of DMSO-d_6 to a solution of [(Cl)FeMBDAP] in $CDCl_3$ leads to the similar spectral pattern (Figure 6, spectrum *F*) indicating formation of a six-coordinated cationic complex [(DMSO-d_6)$_2$FeMBDAP]$^+$ with the α-CH_3 resonance at 55.9 ppm, α-CH_2 at 25.3 ppm, and *meso*-CH at +30.7 ppm. For [(DMSO-d_6)$_2$-FeOEP]$^+$, the α-CH_2 and *meso*-CH resonances appear

(35) Dvornikov, S. S.; Knyukshto, V. N.; Kuzmitski, V. A.; Shulga, A. M.; Solovyov, K. N. *J. Lumin.* **1981**, *23*, 373–392.

(36) Sullivan, E. P, Jr.; Grantham, J. D.; Thomas, C. S.; Strauss, S. H. *J. Am. Chem. Soc.* **1991**, *113*, 5264–5270.

(37) Behere, D. V.; Birdy, R.; Mitra, S. *Inorg. Chem.* **1984**, *23*, 1978–1981.

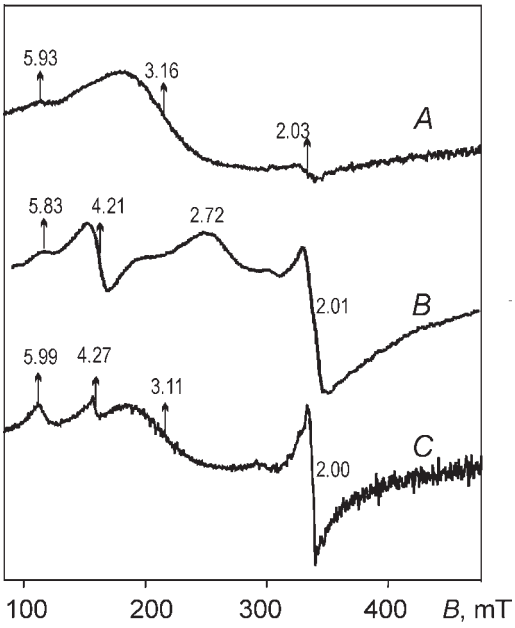

Figure 7. ESR spectra of [(Cl)FeMBDAP] in toluene (*A*), in CH_2Cl_2 (*B*), and in THF (*C*) at 77 K.

at 46.2 and 39 ppm[28,31] and for the monoazaderivative $[(DMSO\text{-}d_6)_2FeOEMAP]^+$ at 29−32 ppm and ca. 36−37 ppm,[11] respectively. These *bis*-DMSO adducts were considered to be high-spin complexes as well as $[(DMSO\text{-}d_6)_2FeTPP]^+$.[37] Due to the large positive charge on Fe, the $d_\pi \rightrightarrows e_g(\pi^*)$ interaction is not possible in these cationic complexes, and an observed downfield shift for the *meso*-CH resonance is determined by combined action of the σ-contact spin delocalization from d_{x2-y2} orbital and the dipole mechanism. For the resonances of α-CH_3 and α-CH_2 groups located in pyrrole rings, some contribution of the $d_\pi \leftleftharpoons e_g(\pi)$ spin delocalization might be also possible.

ESR Measurements. ESR measurements could be accomplished only for the frozen solutions of [(Cl)FeMBDAP] in CH_2Cl_2, THF, and toluene at 77 K. Although the spectra obtained under these conditions are complex and have mediocre quality (see Figure 7 and Figure S1 in the Supporting Information), they are in agreement with the results of ^{1}H NMR and solution magnetic moment measurements and allow some preliminary discussion of the solvent effect on the observed spectral features.

The spectrum in toluene contains the very broad line (ca. 70 mT) at $g = 3.16$, the lower intensity line at $g = 2.03$, and the small shoulder at $g = 5.93$ (Figure 7*A*). The spectra in toluene−CH_2Cl_2 mixture (1:1) and in pure CH_2Cl_2 (Figure 7*B*) are characterized by intense lines at $g \sim 2$ and $g \sim 4.1$−4.3, a shoulder at $g \sim 5.8$−6.0 and a broad line at 2.5−2.8, which disappear in a more diluted solution (see Figure S1 in the Supporting Information). In THF the sharp signals appear at $g = 5.99$, 4.27, and 2.00 along with the broad line at $g \sim 3.1$ (Figure 7*C*). The broad lines in the spectra result evidently from intermolecular spin−spin interactions in solid aggregates which appear due to lowering of solubility and precipitation upon freezing of samples. The signals at $g \sim 4.1$−4.3 and 5.8−6.0 can be assigned to the perpendicular component $g_\perp$ of the g tensor for the predominantly intermediate and high-spin species, respectively. The parallel component $g_\parallel$ in the both species should give the signal at $g \sim 2$. Thus, for the spin-mixed species [(X)FeOEP] (X = ClO_4, SbF_6) in toluene−CH_2Cl_2[34] and for intermediate-spin complexes [(X)FeOETAP] (X = Cl, ClO_4, PF_6, SbF_6) in toluene,[9,10] the $g_\perp$ signal was observed in the 3.8−4.5 range. For the high-spin complex [(Cl)FeOEP], the $g_\perp$-value is 6.14 in toluene−CH_2Cl_2[34] and 6.00 in THF.[14] Usually for the high and spin-mixed [(X)FeOEP] complexes and for intermediate spin [(X)FeOETAP], the $g_\perp$ signal in the low field has higher intensity than the axial component $g_\parallel \sim 2$. It is noteworthy, that the $g \sim 2$ signal in the ESR spectra of [(Cl)FeMBDAP] has higher intensity than the perpendicular components $g_\perp$ in the low field. In the ESR spectrum reported[13,14] for the octaethyl derivative [(Cl)-FeOEDAP] in THF at 77 K the signal observed at $g \sim 2$ was also more intense than the $g_\perp$ line at 5.8−5.9.

The results of the ESR measurements evidence that in the frozen glasses as well as in the crystal state the molecules of [(Cl)FeMBDAP] coexist both in the intermediate- and high-spin states. The spin state of each molecule is determined by its frozen closest solvating surrounding. The spectrum in frozen CH_2Cl_2 is consistent with the presence of the predominantly intermediate-spin species. The observed effective $g_\perp$ value of 4.21 deviates from the theoretical $g_\perp$ value for pure intermediate-spin complexes, indicating the spin-mixed ground state $|\Psi\rangle = a|^6A\rangle + b|^4A\rangle$ with $a^2 + b^2 = 1$. The contribution of the $S = 3/2$ spin state, which can be estimated[38] from the equation $g_\perp = 6a^2 + 4b^2$, is ca. 90%. This estimation is comparable although somewhat lower than could be expected at 77 K from the solution magnetic moment measurements, predicting ca. 87% contribution of the $S = 3/2$ state at 213 K (see Table 2). This discrepancy can be due to differences in H-bonding in liquid and frozen solutions and/or result from uncertainties in determination of the μ_{eff} and $g_\perp$ values. The presence of the minor signal at $g \sim 6$ in the CH_2Cl_2 glass can be explained by some admixture of nonsolvated or other high-spin species. A similar situation was observed for derivatives of $[(ClO_4)FeTPP]$ substituted in the 2,6-positions of phenyl rings—the high-spin signal at $g \sim 6$ even dominated in the ESR spectra recorded in the frozen CH_2Cl_2 glasses, while only intermediate-spin species were seen in CH_2Cl_2 solutions by ^{1}H NMR measurements.[39]

In the THF glass the increased intensity of the high-spin signal with $g_\perp = 5.99$ and the low field shift of the broad signal of an aggregated form to $g \sim 3.1$ are consistent with the presence of the high-spin species in line with the solution ^{1}H NMR and magnetic moment measurements. The signal at $g \sim 4.3$ can be assigned to an admixture of the species forming H-bonds with water traces or to other essentially intermediate spin complexes, most likely $[(THF)_2FeMBDAP]^+$. Similar six-coordinated *bis*-THF adducts $[(THF)_2FeOEP]^+$ and $[(THF)_2FeOEMAP]^+$ are spin-mixed species and also have $g_\perp \sim 4.3$.[40,41] These

(38) Palmer, G. In *Iron Porphyrins*; Lever, A. B. P., Gray, H. B., Eds; Addison-Wesley: Boston, MA, 1983; Part *2*, pp 43−88.

(39) Nesset, M. J. M.; Cai, S.; Shokhireva, T. Kh.; Shokhirev, N. V.; Jacobson, S. E.; Jayaraj, K.; Gold, A.; Walker, F. A. *Inorg. Chem.* **2000**, *39*, 532–540.

(40) (a) Hideki, M.; Tooru, T.; Kenji, O.; Hiroshi, S.; Zenichi, Y.; Hisanobu, Ogoshi *Bull. Chem. Soc. Jpn.* **1982**, *55*, 3891–3895. (b) Kohji, I.; Hiroaki, O.-N.; Noboru, H.; Hideki, M.; Hisanobu, O. *Chem. Phys. Lett.* **1986**, *124*, 401–405.

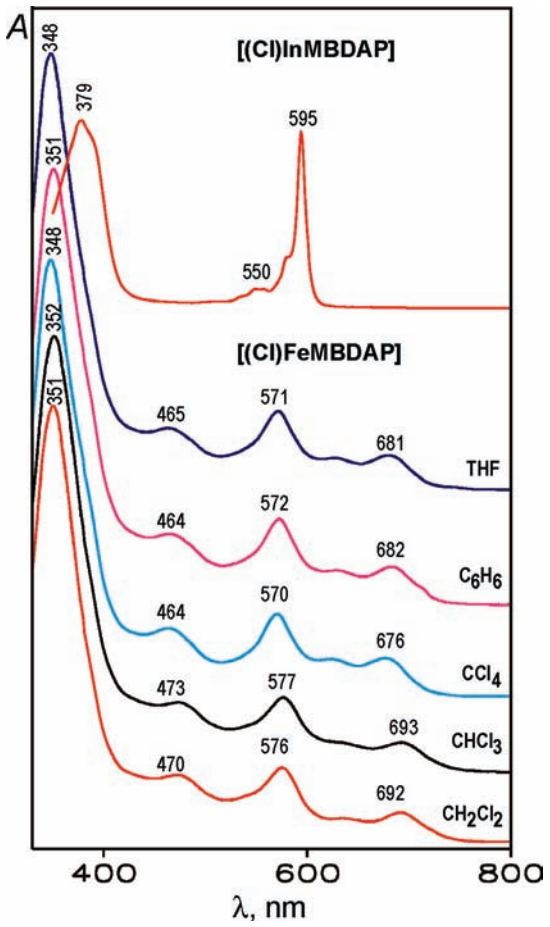

Figure 8. UV−vis spectra of [(Cl)FeMBDAP] in different solvents and of [(Cl)InMBDAP] in CH_2Cl_2.

admixtures, which are observed by ESR measurements in the frozen glasses at 77 K, due to their lower stability and/or rapid dynamic exchange processes at higher temperatures, cannot be seen in the ^{1}H NMR solution spectra. In noncoordinating toluene, no intermediate-spin signal is observed, and the broad line at 3.16 and the shoulder at 5.93 originate from the high-spin species existing mainly in the associated form.

The UV−vis Spectra. The UV−vis spectra of [(Cl)-FeMBDAP] recorded in various noncoordinated solvents are similar to each other (see Figure 8) and contain an intense absorption band in the UV region (ca. 350 nm) and a series of lower intensity bands in the visible region at 465−470, 570−580, 620−630, and 675−695 nm. The maxima of these bands are shifted slightly bathochromically in CH_2Cl_2 and $CHCl_3$ capable to specific solvation of chloride. Such spectral pattern differs strongly from the spectra of the diamagnetic In^{III} complex [(Cl)InMBDAP][17] (see Figure 8) and diazaporphyrin complexes with transition metals having filled d_π orbitals (Zn^{II}, Cu^{II}).[16] The spectrum of these species contains only two bands originating from the singlet $\pi-\pi^*$ transitions which have comparable intensity: the narrow *Q*-band with vibronic satellites in the visible region and the Soret band in the UV region. In the spectra of [(Cl)FeMBDAP], the *Q*-band (570−580 nm) is broadened, and its intensity is strongly decreased in comparison with the Soret band (ca. 350 nm). The maxima of these bands are shifted hypsochromically in comparison with [(Cl)InMBDAP] (379 and 595 nm)[17] or [CuMBDAP] (383 and 586 nm).[16]

This hypsochromic shift of the *Q*-band, the decrease of its intensity and appearance of the new bands in the visible region at 465−470, 620−630 and 675−695 nm, can be associated with the strong interaction of the π-orbitals of the macrocyclic ligand and the half-filled d-orbitals of Fe^{III} in the high- or intermediate-spin state. Interaction with the d_π orbitals rising the LUMOs leads to the hypsochromic shift of the Soret and *Q*-bands. The charge transfer (CT) transitions from the filled π-molecular orbitals of the macrocycle to half-filled d-orbitals can gain intensity. According to theoretical works[42] on the electronic spectra of the five-coordinated Fe^{III} porphyrins, the appearance of the strong CT transitions from highest occupied molecular orbital (HOMO) and HOMO-1 to the d_π orbitals is expected below and above the *Q*-band, respectively. The CT transitions from HOMO-1 to d_{z2} orbitals, which are less mixed, should appear between the *Q*- and Soret bands. Moreover the quartet or sextet states of Fe^{III} mixing with the excited singlet or triplet states of the porphyrin macrocycle can give a number of allowed trip−multiplet transitions. Thus, the theoretical analysis[42a] has shown that in the high- and intermediate-state Fe^{III} porphyrin complexes the trip−sextet and trip−quartet transitions can be responsible for the absorption bands below the *Q*-band, and trip−quartet and trip−doublet transitions might contribute to the absorption between the *Q*- and Soret bands. It was also shown by both theoretical work[42b] and experimental spectra[5,7,34] that the high- and intermediate-spin (spin-mixed) Fe^{III} porphyrins have very similar UV−vis spectra. This is in line with only slight solvent dependence for the UV−vis of [(Cl)FeMBDAP] observed in the present work.

The UV−vis spectra of [(Cl)FeMBDAP] have some resemblance with the spectra of five-coordinated Fe^{III} porphyrins [(X)FeOEP][5,34] and [(X)FeTPP][7] (X = Cl, ClO_4) and monoazaderivative [(Cl)FeOEMAP],[11] but for the diazasubstituted species, the absorption bands in the visible region have higher intensity and are better resolved. Much more similarity is observed with the spectra of the intermediate-spin Fe^{III} tetraazaporphyrins which also have three distinct maxima in the visible region (446, 566, and 684 nm for [(Cl)FeOETAP][10] and 431, 544, and 708 nm for [(Cl)FeOPTAP][43]). Evidently in all cases, the spectral pattern is determined by interaction of the macrocyclic π-orbitals with the d-orbitals of the high/intermediate-spin Fe^{III} atom and by the appearance of the charge−transfer and trip−multiplet transitions. Their complete assignment needs a further special investigation.

High/intermediate-spin six-coordinated complexes $[(L)_2FeMBDAP]^+$ formed in the presence of coordinating DMSO and MeOH also have the spectral pattern (Figure 9) similar to the five-coordinated complex

(41) Nakamura, K.; Ikezaki, A.; Ohgo, Y.; Ikeue, T.; Neya, S.; Nakamura, M. *Inorg. Chem.* **2008**, *47*, 10299–10307.

(42) (a) Zerner, M.; Gouterman, M.; Kobayashi, H. *Theoret. Chim. Acta* **1966**, *6*, 363–400. (b) Edwards, W. D.; Weiner, B.; Zerner, M. C. *J. Phys. Chem.* **1988**, *92*, 6188–6197.

(43) (a) Stuzhin, P. A.; Hamdush, M.; Ziener, U. *Inorg. Chim. Acta* **1995**, *236*, 131–139. (b) Stuzhin, P. A. *Macroheterocycles*, **2009**, *2*, 114−129; http://macroheterocycles.isuct.ru/sites/default/files/MHC2009_t02n02_114-129_0.pdf.

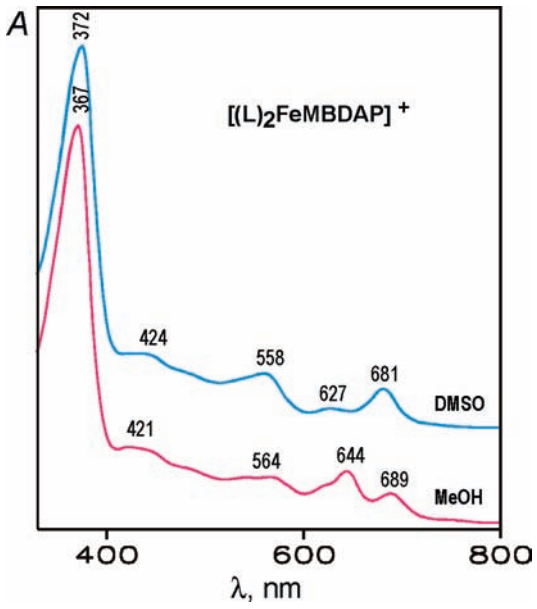

Figure 9. UV−vis spectra of six-coordinated complexes $[(MeOH)_2$-FeMBDAP$]^+$ and $[(DMSO)_2$Fe-MBDAP$]^+$ formed upon dissolution of [(Cl)FeMBDAP] in MeOH and in $CHCl_3$:DMSO 2:1, respectively.

[(Cl)FeMBDAP], and only the positions of the band maxima and their relative intensity are changed. While some spectral differences observed in the visible region are difficult to interpret, the bathochromic shift of the narrow Soret band ($a_{2u}(\pi) \rightarrow e_g(\pi^*)$ transition) in going from five- to six-coordinated complexes is consistent with lower energy of the $a_{2u}(\pi)$ orbital in the five-coordinated complexes due to its interaction with the d_{z2} orbital.

Conclusion

According to theoretical results[2,42b] the intermediate-spin quartet and high-spin sextet states of chloroiron(III) porphyrins are very close in energy which enables their mixing through spin−orbital coupling to form a single state, being a mixture of high- and intermediate-spin states. We have demonstrated that the contribution of the intermediate-spin state in the five-coordinated spin-mixed complexes of Fe^{III} porphyrins can be determined not only by the nature of macrocyclic and axial ligands but also by the solvation of the latter. Our X-ray single-crystal diffraction study, solution ^{1}H NMR, and magnetic and ESR measurements have evidenced that in the chloroiron(III) complex of *meso*-diazasubstituted β-octaalkylporphyrin the Fe^{III} atom exists as predominantly high-spin species ($S = 5/2$) in nonsolvating media (C_6D_6, THF, CCl_4) and has a spin-mixed state ($S = 3/2 \div 5/2$) in the solvents with H-bonding ability ($CHCl_3$, CH_2Cl_2). Specific solvation of axially coordinated chloride anion by H-bonding interaction is favorable for stabilization of the intermediate-spin state. Analysis of the isotropic shifts in the ^{1}H NMR spectra and their temperature dependence provide evidence that *meso*-azasubstitution in the porphyrin ligand stabilizing the $e_g(\pi^*)$ and $a_{2u}(\pi)$ orbitals facilitates the $d_\pi \Rightarrow e_g(\pi^*)$ and diminishes the $d_{z2} \Leftarrow a_{2u}(\pi)$ spin delocalization mechanisms in the five-coordinated high-spin and spin-mixed Fe^{III} complexes.

Peculiar effect of solvation on the spin-state of Fe^{III} revealed in the present work for [(Cl)FeMBDAP] prompted the further study of this and related Fe^{III} complexes of *meso*-azasubstituted porphyrins not only in solution but also for solid samples obtained by crystallization from different solvents using magnetic and spectral (ESR, Mössbauer) measurements at low temperatures up to 4−10 K.

Table 4. Crystallographic Data for the Structural Analysis of [(Cl)FeMBDAP] × $0.5CHCl_3$

empirical formula	$C_{77}H_{101}Cl_5Fe_2N_{12}$
CCDC no.	729 107
T [K]	133(2)
crystal system	triclinic
space group	P-1
a [Å]	12.398(3)
b [Å]	13.190(3)
c [Å]	24.410(8)
α [°]	95.801(5)°
β [°]	94.753(5)°
γ [°]	110.297(4)°
V [Å^3]	3694.8(17)
Z	2
D_{calcd} [g cm^{-3}]	1.334
μ [mm^{-1}]	0.625
F(000)	1568
θ range [°]	1.66−25.00
reflections collected	19 490
independent reflections	12 728 [R(int) = 0.1053]
data/restraints/parameters	12 728/0/869
$R1$, $wR2[I > 2\sigma(I)]^a$	0.0783, 0.1429
$R1$, $wR2$ (all data)^a	0.2196, 0.1960
GoF	1.009
$\Delta\rho$(max), $\Delta\rho$ (min) [e Å^{-3}]	0.539, −0.823

$^a R1 = \Sigma \| F_o| - |F_c \| / \Sigma |F_o|$; $wR2 = (\Sigma[w(F_o^2 - F_c^2)^2] / \Sigma w(F_o^2)^2)^{1/2}$.

Experimental Section

Preparation. The starting compound 2,8,12,18-tetrabutyl-3,7,13,17-tetramethyl-5,10-diazaporphine, H_2MBDAP, and its In^{III} complex [(Cl)InMBDAP] were prepared as described previously.[15,17a]

2,8,12,18-Tetrabutyl-3,7,13,17-tetramethyl-5,10-diazaporphyrinatoiron(III) chloride, [(Cl)FeMBDAP]. Free base H_2MBDAP (30 mg, 0.05 mmol) was refluxed in glacial acetic acid (20 mL) in the presence of iron powder (28 mg, 0.5 mmol) for 3 h. After completion of the reaction (disappearance of the free base absorption bands in the UV−vis spectrum), the reaction mixture was mixed with an equal volume of $CHCl_3$, filtrated, washed twice with water to remove acetic acid, treated with aqueous 15% HCl solution, washed again with water, and dried over anhydrous Na_2SO_4. Addition of hexane lead to black-brown needles which were dried at 80 °C under vacuum (yield 25 mg, 75%). IR (KBr) ν/cm^{-1}: 2952 s, 2928 s, 2859 s, 1455 s, 1376 s, 1155 s, 985 m, 922 m, 856 m, 761 m, 750 s, 715 w. UV−vis λ_{max}/nm (lgε), $CHCl_3$: 350 (4.94), 473 (4.16), 575 (4.21), 639 (3.70), 692 (3.82); Anal. calcd for $C_{38}H_{50}ClFeN_6$ (682.15): C, 66.91; H, 7.39; N 12.32. Found: C, 66.72; H, 7.56; N 12.05. ^{1}H NMR spectra are presented in Figure 3 and tabulated in Table 3.

Solution and Refinement of the Structure. X-ray structure analysis of [(Cl)FeMBDAP] × $0.5CHCl_3$: Bruker SMART Apex II diffractometer (CCD-detector, Mo Kα radiation λ = 0.71073 Å, graphite monochromator, x-scanning) at 120(2) K. Corrections for absorption were made by SADABS.[44] The structure was solved by the direct method and refined by the full-matrix least-squares method for F^2 with anisotropic parameters for all non-hydrogen atoms. All calculations were performed with the use of the SAINT[45] and SHELXTL-97[46] program packages.

(44) Sheldrick, G. M. *SADABS*; Bruker AXS Inc.: Madison, WI, 1997.
(45) *SMART V5.051 and SAINT V5.00*, Area detector control and integration software; Bruker AXS Inc.: Madison, WI, 1998.
(46) Sheldrick, G. M. *SHELXTL-97*, V5.10; Bruker AXS Inc.: Madison, WI, 1997.

Crystallographic details are given in Table 4, and selected bond distances in the caption to Figure 1.

Instrumentation and Measurements. ^{1}H NMR spectra were recorded on a Bruker Avance-500 Spectrometer using deuterated solvents purchased from Aldrich. The Evans method[23] has been used for measurement of effective magnetic moments μ_{eff} in solution from the difference of the chemical shifts of the residual protons of the deuterated solvent in the pure solvent (δ_0) and in the solution of the complex (δ_i) with concentration m (g/mL). The values of mass susceptibilities χ_i were calculated using the equation valid for the field direction in the superconducting magnets:[24]

$$\chi_i = -\frac{3}{4\pi}\frac{(\delta_0 - \delta_i)}{m} + \chi_{solv}$$

where χ_{solv} is the mass susceptibility of the solvent. The calculated molar susceptibility χ_M was corrected for diamagnetism using the Pascal constants ($\chi_{dia} = -4.01 \times 10^{-4}$), and the effective magnetic moment μ_{eff} was then calculated using the equation:

$$\mu_{eff} = 2.8279\sqrt{\chi_M T}$$

In the low-temperature measurements, correction was also made for the temperature dependence of the solvent density.[47]

UV−vis spectra were registered using a Hitachi U-2000 spectrophotometer, ESR spectra were recorded on a Bruker E-680 X "Elexsys" spectrometer, and IR spectrum was measured on an Avatar 360 FT-IR ESP spectrometer. Elemental analysis was performed on CHNS-O Analyzer Flash EA 1112 Fa. Thermo Quest.

Acknowledgment. This work was supported by Russian Foundation for Basic Research.

Supporting Information Available: X-ray data for [(Cl)-FeMBDAP] × 0.5$CHCl_3$ (CIF), tables of crystallographic and structural refinement data, and Figure S1 illustrating concentration dependence of ESR spectra (PDF). This material is available free of charge via the Internet at http://pubs.acs.org.

(47) Karapetyan, Yu. A.; Eichis, V. N. *Physico-chemical properties of non-aqueous electrolite solutions*. Khimiya: Moscow, 1989; 256 p. (in Russ).